Crystal-field determination for trivalent thulium in yttrium orthoaluminate

J. M. O'Hare
Department of Physics, University of Dayton, Dayton, Ohio 45469

V. L. Donlan
AFML, Wright-Patterson Air Force Base, Dayton, Ohio 45433

(Received 15 March 1976)

The polarized absorption spectra of $YAlO_3:Tm^{3+}$ were analyzed at 77°K. A free-ion calculation was performed by fitting the centers of gravity of the J manifolds. The coefficients which gave the best least-squares deviation of the calculated "free-ion" spectra from the observed "free-ion" spectra were $E^1 = 7075.5$, $E^2 = 33.8$, $E^3 = 654.3$, $\zeta = 2631.8$, $\alpha = 8.0$, $\beta = -764.9$; where all parameters have units of cm^{-1}. A crystal-field calculation was also carried out by fitting Stark splittings and irreducible representations to the observed spectra. In order to obtain good starting parameters for fitting a C_s (C_{1h}) symmetry Hamiltonian, a descending symmetries technique was used. The results of a least-squares fit of the crystal-field Hamiltonian to the observed $^3F_4$, $^3F_3$, $^1G_4$, and $^1D_2$ Stark splittings gave the following parameters for the C_s Hamiltonian: $B_0^2 = -434.9$, $\mathrm{Re}B_2^2 = 420.8$, $\mathrm{Im}B_2^2 = 199.4$, $B_0^4 = -691.6$, $\mathrm{Re}B_2^4 = 444.9$, $\mathrm{Im}B_2^4 = 114.2$, $\mathrm{Re}B_4^4 = 501.2$, $\mathrm{Im}B_4^4 = -389.2$, $B_0^6 = -260.4$, $\mathrm{Re}B_2^6 = 175.6$, $\mathrm{Im}B_2^6 = 229.7$, $\mathrm{Re}B_4^6 = 92.7$, $\mathrm{Im}B_4^6 = 542.4$, $\mathrm{Re}B_6^6 = 410.5$, $\mathrm{Im}B_6^6 = 113.4$; where all units are in cm^{-1}.

I. INTRODUCTION

The spectrum of Tm^{3+} in $YAlO_3$ has been investigated by Weber and co-workers,[1] by Hobrock,[2] and by Antonov *et al.*[3] In this paper we present some additional data and complete J-mixed crystal-field calculations for the Tm^{3+} ion in $YAlO_3$. Weber *et al.*[1] have studied absorption and emission intensities of several rare earths in $YAlO_3$ in order to determine oscillator strengths. Hobrock[2] and Antonov *et al.*[3] have determined the Stark components of all of the J manifolds except $^1I_6$, $^3P_0$, $^3P_1$, $^3P_2$, and $^1S_0$ which lie in the absorption band of $YAlO_3$. Hobrock has also determined the irreducible representations of the $^3F_4$, $^3F_3$, $^3F_2$, $^1G_4$, and $^1D_2$ manifolds by means of polarized absorption measurements. We have remeasured these manifolds and for the most part we agree with Hobrock.[2] We have, however, made some changes in the assignments of a few of the irreducible representations and the Stark levels. We have used these measurements to do fully J-mixed crystal-field calculations for Tm^{3+} in $YAlO_3$.

$YAlO_3$ has the gadolinium-orthoferrite structure, belonging to the orthorhombic space group $D_{2h}^{16}(Pbnm)$.[4] Rare-earth ions enter the $YAlO_3$ lattice substitutionally at the Y^{3+} sites. The sites have the point-group symmetry C_s ($C_s = C_{1h}$).[2]

In the calculations, a "free-ion" Hamiltonian was fit to the centers of gravity of the J manifolds. The resulting free-ion intermediate coupled eigenvectors were then used in the crystal-field calculations. Since the Tm^{3+} ion occupies a site of C_s symmetry, certain difficulties occur in attempting any meaningful crystal-field calculation due to the large number of crystal-field coefficients. The procedure used here was the technique of descending symmetries[5] whereby the observed C_s spectra were extrapolated to the O_h symmetry spectra of an ideal perovskite structure. The symmetry was then reduced to C_s by a series of perturbations consisting of distortions from the ideal perovskite structure. This was accomplished by first imagining the O_h site symmetry perturbed to D_{4h} by contracting the c axis of the $YAlO_3$ pseudocell. One can then imagine the symmetry is distorted to D_{2h} by changing the β angle of the pseudocell to 91.6°. Finally C_s symmetry is achieved by slightly displacing the Tm^{3+} ion and the surrounding O^{2-} ions.

II. THEORY

A. Free ion

The ground configuration of trivalent rare-earth ions (R^{3+}) is $(Xe)4f^N$. The Hamiltonian of the free ion can be accurately represented by effective operators which include Coulomb, spin-orbit, configuration interaction, spin-spin, and spin–other-orbit interactions. In general the effective free-ion Hamiltonian for the incomplete f^N shell can be written

$$H = E^1\epsilon_1 + E^2\epsilon_2 + E^3\epsilon_3 + \xi\sum_i \vec{s}_i \cdot \vec{l}_i + \alpha L(L+1) + \beta G(G_2) + \gamma G(R_7) + H_{ss}(M^0, M^2, M^4)$$
$$+ H_{soo}(M^0, M^2, M^4) + H_{oo}(M^0, M^2, M^4) + H_{ci}(P^2, P^4, P^6) + \sum_{\substack{i=2 \\ i\neq 5}}^{8} t_i T^i . \quad (1)$$

The first three terms are the electrostatic interaction cast in a form due to Racah.[6] The E^k's are combinations of Slater integrals which are treated as adjustable parameters and the ϵ_k's are angular operators which have been tabulated by Nielson and Koster.[7] The fourth term, $\xi\sum_i \vec{s}_i \cdot \vec{l}_i$, is the spin-orbit interaction with ξ being an adjustable parameter. The next three terms are two-body configuration-interaction terms; α, β, and γ are adjustable parameters and $G(G_2)$ and $G(R_7)$ are eigenvalues of Casimir's operator for the groups G_2 and R_7.[5] The terms H_{ss}, H_{soo}, and H_{oo} stand for spin-spin, spin–other-orbit, and orbit-orbit interactions. They are functions of M^0, M^2, and M^4 which are the so called Marvin's integrals.[8] The Marvin's integrals are treated as adjustable parameters. The term H_{ci} is the electrostatically correlated spin-orbit interaction.[9,10] The quantities P^2, P^4, and P^6 are essentially radial integrals which are treated as adjustable parameters. The remaining terms in the Hamiltonian are the effective three-body interactions.[11]

The matrix of the free-ion Hamiltonian in the Russell-Saunders basis can be diagonalized to obtain the intermediate coupled eigenvectors. The diagonalization is carried out several times by iteratively varying the adjustable parameters to minimize the rms deviation,

$$\left(\sum_{i=1}^{n}\frac{(E_e^i - E_c^i)^2}{n-p}\right)^{1/2}, \quad (2)$$

where E_e^i is the center of gravity of the ith experimental manifold, E_c^i is the calculated energy, n is the number of experimental centers of gravity used in the fit, and p is the number of parameters varied. The number of adjustable parameters which can be fit is constrained by the number of experimental centers of gravity available. For $YAlO_3$:Tm^{3+} only E^1, E^2, E^3, ξ, α and β could be used. The "best-fit" parameters, i.e., those giving the minimum rms deviation for Eq. (2), are then used to generate intermediate coupled eigenvectors for use in the crystal-field calculations.

B. Crystal field

The site symmetry of the Tm^{3+} ion in $YAlO_3$ is C_s. The C_s point group (C_{1h}) contains only two symmetry operations, I and σ_h, the identity element and a reflection through the horizontal plane. The perturbation Hamiltonian for a crystal field of this symmetry involves complex coefficients and can be written

$$H_{CF} = \sum_{j=1}^{N} V_j , \quad (3)$$

$$V_j = [B_0^2 C_0^2 + \mathrm{Re}B_2^2(C_2^2 + C_{-2}^2) + i\,\mathrm{Im}B_2^2(C_2^2 - C_{-2}^2) + B_0^4 C_0^4 + \mathrm{Re}B_2^4(C_2^4 + C_{-2}^4)$$
$$+ i\,\mathrm{Im}B_2^4(C_2^4 - C_{-2}^4) + \mathrm{Re}B_4^4(C_4^4 + C_{-4}^4) + i\,\mathrm{Im}B_4^4(C_4^4 - C_{-4}^4) + B_0^6 C_0^6 + \mathrm{Re}B_2^6(C_2^6 + C_{-2}^6) + i\,\mathrm{Im}B_2^6(C_2^6 - C_{-2}^6)$$
$$+ \mathrm{Re}B_4^6(C_4^6 + C_{-4}^6) + i\,\mathrm{Im}B_4^6(C_4^6 - C_{-4}^6) + \mathrm{Re}B_6^6(C_6^6 + C_{-6}^6) + i\,\mathrm{Im}B_6^6(C_6^6 - C_{-6}^6)]_j , \quad (4)$$

where

$$(C_q^k)_j = [4\pi/(2k+1)]^{1/2} Y_{kq}(\theta_j, \phi_j) \quad (5)$$

and

$$B_q^k = -\left(\frac{4\pi}{2k+1}\right)(l|r^k|l)\sum_j \frac{Z_j e^2}{R_j^{k+1}} Y_{kq}^*(\theta_j, \phi_j) \quad (6)$$

in the point-charge model. The Y_{kq} are spherical harmonics and $\sum_j$ stands for a lattice sum. Z_j is the charge on the jth lattice ion and R_j is the separation between the R^{3+} impurity and the jth lattice ion. The matrix elements of this Hamiltonian in the intermediate coupled basis are of the form[5]

$$(f^n \alpha SLJJ_z|B_q^k C_q^k|f^n \alpha' S'L'J'J_z') = B_q^k \delta(S,S')(l\|C^k\|l)(-1)^{J-J_z}\begin{pmatrix} J & k & J' \\ -J_z & q & J_z' \end{pmatrix}(-1)^{S+L'+J+k}\begin{Bmatrix} J & J' & k \\ L' & L & S \end{Bmatrix}$$
$$\times [J,J']^{1/2}(f^n \alpha SL\|U^{(k)}\|f^n \alpha' S L'), \quad (7)$$

where the reduced matrix elements are given by Nielson and Koster.[7]

It is well known that Eq. (6) is inadequate for calculation of the B_q^k's, these coefficients are, instead, treated as adjustable parameters to give the best fit to the empirical data. The complete specification of the crystal field of $YAlO_3:R^{3+}$ requires the fitting of 15 B_q^k parameters. Only 14 of these parameters are independent; thus the number of parameters to be fit could be reduced to 14 by a suitable rotation about the z axis. To obtain a physically "true" solution with so many parameters is improbable unless supplementary information besides the Stark levels is available.[12-14] The reason for this is that the minimization of Eq. (2), where the E_e^i and E_c^i refer to the respective splittings of the experimental and calculated Stark levels from their mainifold centers of gravity, with so many adjustable parameters will yield different local minima, depending upon the initial choices for the B_q^k's. It is thus difficult to determine which is a true or physically realistic minimum.

Since Tm^{3+} is an even electron system, polarized absorption spectra allow one to also identify the irreducible representations of the Stark levels. In C_s symmetry there are two irreducible representations, Γ_1 and Γ_2, for even electron systems. This, along with the descending symmetries approach which yields starting values for the B_q^k's, was used to determine the best fit to the crystal-field spectra.

C. Descending symmetries

A mechanism for finding physically significant crystal-field coefficients for low-symmetry sites is the method of descending symmetries.[5] This consists of regarding the low-symmetry crystal field as being made up of components of higher symmetry fields. For example, in some rare-earth garnets the crystal field can be regarded as predominantly cubic O_h with small distortion to C_{2v}.[15] In the rare-earth ethylsulfates the point symmetry at the rare-earth ion is C_{3h}, however, it has been more useful to regard the crystal field as being almost entirely composed of the slightly higher symmetry D_{3h} field.[16] Koningstein and Geusic,[17] in fitting the spectra Nd^{3+} in YAlG, attempted to approximate a D_2 symmetry site by a higher symmetry D_{4h} field. Morrison, Wortman, and Karayianis[18] have recently shown that D_{2h} symmetry more accurately represents the dominant higher symmetry component of the crystal field of Nd^{3+} in YAlG.

In fitting the C_s Hamiltonian, Eq. (4), the starting values for the adjustable parameters B_q^k were determined by the descending symmetries approach. The observed C_s Stark spectra were projected to the O_h symmetry spectra of an ideal perovskite structure. The sequence of irreducible representation labels for the symmetry reductions of O_h to C_s is indicated in Table I. An O_h symmetry Hamiltonian

$$V_j = B_0^4[C_0^4 - (\tfrac{5}{14})^{1/2}(C_4^4 + C_{-4}^4)] + B_0^6[C_0^6 + (\tfrac{7}{2})^{1/2}(C_4^6 + C_{-4}^6)] \quad (8)$$

was fit to these projected spectra. Only the $^1G_4$ manifold was used in this O_h fit, since its spectrum was not complicated by level crossing under subsequent symmetry reductions. The O_h symmetry was then imagined to be distorted to D_{4h}, the O_h Stark spectrum projected to a D_{4h} spectrum, and the D_{4h} spectrum fit to a D_{4h} Hamiltonian,

$$V_j = B_0^2C_0^2 + B_0^4C_0^4 + B_4^4(C_4^4 + C_{-4}^4) + B_0^6C_0^6 + B_4^6(C_4^6 + C_{-4}^6). \quad (9)$$

Next the D_{4h} spectrum was projected to D_{2h} by imagining the pseudo cell distorted to D_{2h} symmetry and the projected D_{2h} spectrum was fit to a D_{2h} Hamiltonian,

$$V_j = B_0^2C_0^2 + B_2^2(C_2^2 + C_{-2}^2) + B_0^4C_0^4 + B_2^4(C_2^4 + C_{-2}^4) + B_4^4(C_4^4 + C_{-4}^4) + B_0^6C_0^6 + B_2^6(C_2^6 + C_{-2}^6) + B_4^6(C_4^6 + C_{-4}^6) + B_6^6(C_6^6 + C_{-6}^6). \quad (10)$$

Finally the B_q^k's obtained in fitting the projected D_{2h} spectra were used as starting parameters in fitting the observed Stark spectra to the C_s Hamiltonian, Eq. (4).

The ratios, B_4^4/B_0^4 and B_4^6/B_0^6, in the O_h Hamiltonian, Eq. (8), are of opposite sign to what is customary.[5] This simply expresses the fact that all calculations are referred to the crystallographic axes rather than the axes of the pseudocell, which are rotated about the z axis by 45° from the crystallographic axes (see, e.g., Figs. 1 and 2). The form of the C_s Hamiltonian is independent of the orientation of the x-y axis. One of the imaginary coefficients of Eq. (4) could be arbitrarily set equal to zero; this would amount to a rotation about the z axis. However, in this calculation the C_s parameters are obtained by using the coeffi-

TABLE I. Compatibility tables for the groups O_h, D_{4h}, D_{2h} and C_s (Ref. 28).

$O_h \rightarrow D_{4h}$	$D_{4h} \rightarrow D_{2h}$	$D_{2h} \rightarrow C_s$
$^1\Gamma_1 \rightarrow {}^1\Gamma_1$	$^1\Gamma_1 \rightarrow {}^1\Gamma_1$	$^1\Gamma_1 \rightarrow {}^1\Gamma_1$
$^1\Gamma_2 \rightarrow {}^1\Gamma_3$	$^1\Gamma_2 \rightarrow {}^1\Gamma_3$	$^1\Gamma_2 \rightarrow {}^1\Gamma_2$
$^2\Gamma_3 \rightarrow {}^1\Gamma_1 + {}^1\Gamma_3$	$^1\Gamma_3 \rightarrow {}^1\Gamma_1$	$^1\Gamma_3 \rightarrow {}^1\Gamma_1$
$^3\Gamma_4 \rightarrow {}^1\Gamma_2 + {}^2\Gamma_5$	$^1\Gamma_4 \rightarrow {}^1\Gamma_3$	$^1\Gamma_4 \rightarrow {}^1\Gamma_2$
$^3\Gamma_5 \rightarrow {}^1\Gamma_4 + {}^2\Gamma_5$	$^2\Gamma_5 \rightarrow {}^1\Gamma_2 + {}^1\Gamma_4$	

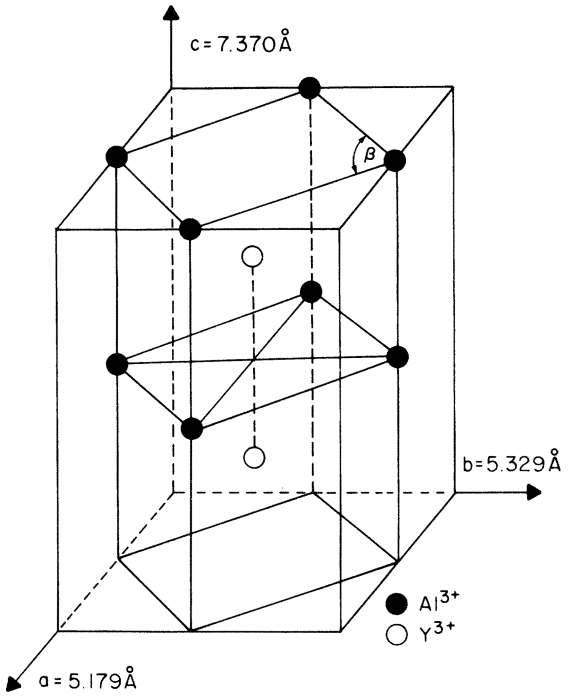

FIG. 1. Unit cell of yttrium orthoaluminate.

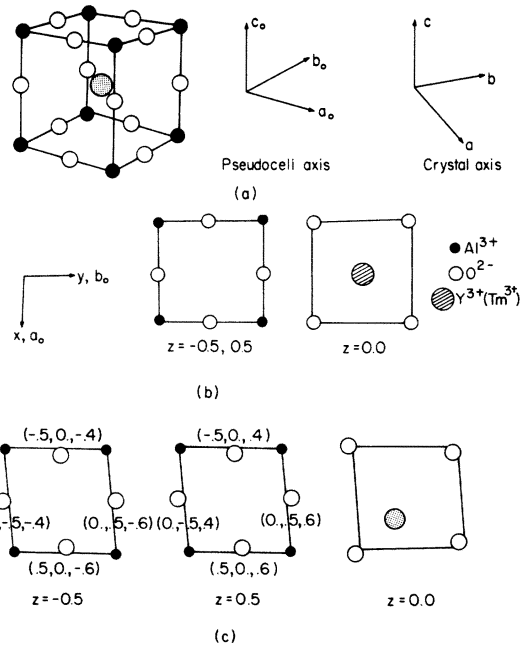

FIG. 2. (a) Relative orientation of crystal axis and pseudocell axis in $YAlO_3$. (b) The $YAlO_3$ pseudocell in the cubic approximation, $a_0 = b_0 = c_0 = 3.71$ Å and $\alpha = \beta = \gamma = 90°$. In the D_{4h} approximation, $a_0 = b_0 \neq c_0 = 3.685$ Å and $\alpha = \beta = \gamma = 90°$. In the D_{2h} approximation, $a_0 = b_0 \neq c_0 = 3.685$ Å and $\beta = 91.6°$. The two rightmost figures show X-Y planes at $Z = -\frac{1}{2}$, $\frac{1}{2}$, and 0 in the cubic approximation. (c) X-Y planes of the $YAlO_3$ pseudocell with C_s symmetry, $a_0 = b_0 \neq c_0$, $\beta = 91.6°$, and the Y^3 ion and O^{2-} ions displaced.

cients of a higher-symmetry Hamiltonian D_{2h} as starting parameters. The higher-symmetry Hamiltonians are referred to a specific orientation of the x-y axis, namely the crystallographic axes. It is therefore more consistent, in this case, to fit all 15 C_s parameters.

Figure 2 shows the physical distortions of the ideal perovskite pseudocell that were envisioned in proceeding from O_h to D_{4h} to D_{2h} to C_s symmetry.

III. EXPERIMENTAL

Two crystals of $YAlO_3$ nominally doped with 0.05 and 0.5 mole% Tm^{3+} were purchased from Lambda/Airtron. The dimensions of the crystals were 17 $\times 11 \times 12$ mm^3 parallel to the a, b, and c crystallographic axis, respectively.

The absorption spectra were taken on a Jarrell-Ash 3.4-m focal length, Ebert-Fastie mount, grating spectrograph. A grating of 590 groves/mm blazed at 4000 Å in first order was used which gives a reciprocal linear first order dispersion of 5 Å/mm. The instrument was operated in both the photographic and photoelectric recording modes. In the photographic mode the spectra were recorded on V-F and I-N Kodak photographic plates. The photographic plates were scanned on a Joyce-Loebl Mark IIB microdensitometer. Position measurements of the spectroscopic features to better than 10 μm on the plate can be reproduced on this instrument. For the photoelectric recording modes, a RCA Quantacon C31025C photomultiplier, permitting operation from 2000 to 9000 Å, was used. Electronic signal processing was accomplished by lock-in techniques using a PAR model HR-8 lock-in amplifier. The output of the lock-in was displayed on a strip-chart recorder.

In all experiments, the crystals were cooled to 77 °K using a variable-temperature Air Products and Chemicals liquid transfer helitron refrigeration model LT-3-110. The light sources for the absorption measurements were a 200-W quartz-iodine tungsten lamp and a Hanovia type 977-B1, 900-W Osram high-pressure compact-arc Xe lamp. A Westinghouse Fe-Ne hollow cathode lamp was used for wavelength calibration. A Glan-Thomson polarizer was used to obtain the polarized absorption spectra.

IV. RESULTS

A. Absorption measurements

We have measured the polarized absorption spectra of the $^3F_4$, $^3F_3$, $^3F_2$, $^1G_4$, and $^1D_2$ mani-

folds of $YAlO_3$: Tm^{3+}. Hobrock[2] has found that the two lowest Stark components of the $^3H_6$ ground manifold were separated by only 3.1 cm^{-1} and were Γ_2 and Γ_1 states with Γ_2 being the lowest. Thus all transitions from the ground state appeared in pairs except for some lines which were too broad to resolve. Polarized absorption measurements distinguish between these pairs and allow the irreducible representations of the excited states to be identified. The results of our measurements along with those of Hobrock and Antonov *et al*. are presented in Table II. We did not attempt to remeasure the $^3H_6$, $^3H_4$, and $^3H_5$ manifolds since we were primarily interested in manifolds for which we could obtain the irreducible representations of all of the Stark components in order to do the crystal-field calculations.

Of the manifolds that we measured, we essentially agree with Hobrock[2] on the values of the Stark components with the exception of one line in the $^3F_2$ manifold C_2 and one line in the $^1G_4$ manifold D_4. In addition, we disagree on the assignment of the irreducible representation for four of the $^1G_4$ lines and two of the $^1D_2$ lines. We also disagree on the assignments of two of the irreducible representations for the $^3F_2$ manifolds. However, our polarized absorption spectra for this manifold was not well defined except for the lines C_2 and C_4.

B. Free-ion measurements and calculations

The free-ion Hamiltonian which was fit to the observed centers of gravity in $YAlO_3$: Tm^{3+} is

$$H = E^1\epsilon_1 + E^2\epsilon_2 + E^3\epsilon_3 + \xi \sum_{i=1}^{n} \vec{l}_i \cdot \vec{s}_i + \alpha L(L+1) + \beta G(G_2). \tag{11}$$

Since Tm^{3+} is an f^{12} configuration, there are no three body interactions. Also, only eight J manifolds can be observed in absorption and fluorescence since the $^1I_6$, $^3P_0$, $^3P_1$, $^3P_2$, and $^1S_0$ manifolds lie in the absorption band of $YAlO_3$. Thus the last six terms in Eq. (1) are not included in the fit. The γ parameter cannot be evaluated since it is predominantly determined by the position of the $^1S_0$ manifold.[19] The results of the free ion calculations are presented in Table III.

C. Crystal-field calculations

The $^1G_4$ manifold appeared to be the most straightforward for uniquely relating the C_s spectra to the higher-symmetry irreducible representation labels. For this reason, only the $^1G_4$ multiplet was fit in the O_h calculation. A negative value for the cubic B_0^4 coefficient produces an ordering of the cubic irreducible representation labels shown in Fig. 3. A positive value of the cubic B_0^4 coefficient, on the other hand, produces the following ordering of the cubic irreducible representation labels: Γ_5, Γ_3, Γ_4, and Γ_1 with Γ_5 being the lowest in energy. It can be seen from considerations of Tables I and II that there is not any combination of C_s $^1G_4$ states which can produce such an ordering. Thus the projection shown in Fig. 3 appears to be the only possibility for the $^1G_4$ manifold. The values of B_0^4 and B_0^6 obtained in this fit were $B_0^4 = -1128.2$ cm^{-1} and $B_0^6 = 27.9$ cm^{-1}. The rms deviation between the projected and calculated spectrum was 13.4 cm^{-1}. In fitting the projected and calculated spectra, splittings from the centers of gravity rather than the values of the Stark components themselves were used. In addition, although only the projected and calculated Stark splittings for the $^1G_4$ manifold were fit, the Stark components of all manifolds were included in the basis. This means that, for Tm^{3+}, the basis consists of 91 $|LSJM_J\rangle$ states. Thus all of the crystal-field calculations were fully J mixed. Also, in fitting the splittings from the center of gravity, Eq. (2) was modified to be

$$\left(\sum_{i=1}^{n} \alpha_i \frac{[E_c^i(\Gamma_i) - E_c^i(\Gamma_i)]^2}{n-p} \right)^{1/2}, \tag{12}$$

where α_i is the degeneracy of the state Γ_i. Thus the fitting procedure was constrained to match not only the energy levels of the observed states but also their irreducible representation labels. This fitting procedure was used in all of the calculations described below.

After the cubic fit, the projected O_h Stark spectrum of the $^1G_4$ manifold was projected to the spectrum of a D_{4h} symmetry site and the splittings fit by a D_{4h} Hamiltonian, Eq. (9). This would result if the c axis of the ideal perovskite cubic cell were changed. The starting parameters for this calculation were those obtained from the cubic calculation above. Only the B_0^2 parameter was allowed to vary while the B_0^4, B_4^4, B_0^6, and B_4^6 parameters were held at their cubic values. The rationale for holding these parameters fixed was the assumption that each successive symmetry change could be achieved by a small perturbation. Also, the primary objective of the D_{4h} calculation was to determine the sign of the B_0^2 coefficient which came closest to reproducing the order of the D_{4h} irreducible representation labels for the projection shown in Fig. 3. The starting value for B_0^2 was zero and the final value obtained in this phase of the calculation was $B_0^2 = -856.6$ cm^{-1} with an rms deviation of 34.7 cm^{-1}.

Next the D_{4h} spectrum of the $^1G_4$ manifold was projected to D_{2h}. This would correspond to changing the β angle (cf. Fig. 2) to a value other than

TABLE II. Observed energy levels of Tm^{3+} in $YAlO_3$.

Multiplet	Empirical label	Ref. 3 Energy (cm^{-1})	Ref. 2 Energy (cm^{-1})	C_s Rep	This work Energy (cm^{-1})	This work C_s Rep
$^3H_6$	Z_1	0	0.0	Γ_2		
	Z_2	70	3.1	Γ_1		
	Z_3	144	66.1			
	Z_4	214	111.0			
	Z_5	243	236.1			
	Z_6	288	261.1			
	Z_7	319	270.3			
	Z_8	409	284.0			
	Z_9	445	308.0			
	Z_{10}	472 [a]	316.8			
	Z_{11}	574	321.9			
	Z_{12}	596 [a]	349.5			
	Z_{13}	628				
$^3H_4$	Y_1	5631	5622.2			
	Y_2	5719	5626.9			
	Y_3	5729	5714.0			
	Y_4	5825	5725.8			
	Y_5	5894	5820.4			
	Y_6	5919	5840.5			
	Y_7	5940	5929.1			
	Y_8	5968	5961.0			
	Y_9	5988	5987.8			
$^3H_5$	X_1	8263	8260.8	Γ_2		
	X_2	8323	8265.1	Γ_1		
	X_3	8344	8322.2	Γ_2		
	X_4	8377 [a]	8345.1	Γ_1		
	X_5	8463	8376.4			
	X_6	8485	8458.6			
	X_7	8535	8482.3			
	X_8	8553	8564.3			
	X_9	8562	8588.7			
	X_{10}	8596 [a]	8599.2			
	X_{11}	8596 [a]	8690.3			
$^3F_4$	A_1	12 510	12 518.9	Γ_1	12 514.5	Γ_1
	A_2	12 572	12 576.5	Γ_2	12 573.9	Γ_2
	A_3	12 662	12 668.7	Γ_1	12 667.4	Γ_1
	A_4	12 739	12 745.3	Γ_1	12 742.3	Γ_1
	A_5	12 780	12 786.6	Γ_2	12 783.4	Γ_2
	A_6	12 881	12 870.2	Γ_2	12 872.2	Γ_2
	A_7	12 909 [a]	12 886.0	Γ_2	12 884.6	Γ_2
	A_8	12 938	12 912.5	Γ_1	12 909.8	Γ_1
	A_9	12 947	12 949.4	Γ_1	12 950.6	Γ_1
$^3F_3$	B_1	14 454	14 448.1	Γ_1	14 448.2	Γ_1
	B_2	14 483	14 478.0	Γ_2	14 478.2	Γ_2
	B_3	14 518	14 511.4	Γ_2	14 512.9	Γ_2
	B_4	14 556	14 547.0	Γ_2	14 552.2	Γ_2
	B_5	14 595	14 594.0	Γ_1	14 592.9	Γ_1
	B_6	14 609	14 608.4	Γ_1	14 606.3	Γ_1
	B_7	14 623	14 624.5	Γ_2	14 622.3	Γ_2
$^3F_2$	C_1	15 030	15 024.3	Γ_1	15 026.6	(Γ_1) [b]
	C_2	15 096	15 063.8	Γ_2	15 088.2	Γ_2
	C_3	15 195	15 181.4	Γ_1	15 177.5	(Γ_2)
	C_4	15 292	15 190.8	Γ_1	15 193.4	Γ_1
	C_5	15 309 [a]	15 289.2	Γ_2	15 285.2	(Γ_1)

TABLE II. *(continued)*

Multiplet	Empirical label	Ref. 3 Energy (cm^{-1})	Ref. 2 Energy (cm^{-1})	C_s Rep	This work Energy (cm^{-1})	C_s Rep
$^1G_4$	D_1	21 028	21 020.5	Γ_1	21 019.7	Γ_1
	D_2	21 108	21 101.6	Γ_1	21 100.9	Γ_1
	D_3	21 204	21 192.7	Γ_2	21 193.4	Γ_2
	D_4	21 300	21 201.2	Γ_2	21 220.5	Γ_1
	D_5	21 329	21 292.0	Γ_1	21 293.4	Γ_2
	D_6	21 463	21 321.6	Γ_1	21 320.8	Γ_1
	D_7	21 495	21 453.2	Γ_2	21 455.2	Γ_2
	D_8	21 628	... [c]	Γ_1	21 542.2	Γ_2
	D_9		21 617.5	Γ_2	21 620.4	Γ_1
$^1D_2$	E_1	27 700 [a]	27 686.3	Γ_1	27 693.0	Γ_2
	E_2	27 848	27 705.9	Γ_2	27 708.4	Γ_1
	E_3	27 902 [a]	27 838.7	Γ_1	27 843.6	Γ_1
	E_4	28 007 [a]	27 894.4	Γ_2	27 901.8	Γ_2
	E_5	28 179 [a]	27 926.4	Γ_1	27 926.3	Γ_1

[a] Antonov *et al.* indicate that these levels were not well defined in their spectra.

[b] The assignments enclosed in parenthesis are lines for which our polarized absorption data did not allow unambiguous assignments to be made, either because both π and σ components were not observed or the line was too broad to be clearly resolved.

[c] This line appears to be a misprint in Hobrock's thesis (Ref. 2).

TABLE III. Comparison of calculated and experimental centers of gravity of $YAlO_3:Tm^{3+}$.

Free-ion manifold	Expt. center of gravity E_e (cm^{-1}) [a]	Calc. free-ion energy E_c (cm^{-1}) [b]	$E_e - E_c$ (cm^{-1})
$^3H_6$	210.6	228.4	−17.8
$^3H_4$	5803.1	5791.6	11.5
$^3H_5$	8436.6	8430.9	5.7
$^3F_4$	12 766.5	12 741.1	25.4
$^3F_3$	14 544.7	14 557.6	−12.9
$^3F_2$	15 154.2	15 154.5	− 0.3
$^1G_4$	21 307.4	21 319.0	−11.6
$^1D_2$	27 814.6	27 814.6	0.0
$^1I_6$		34 375.2	
$^3P_0$		35 031.9	
$^3P_1$		35 686.7	
$^3P_2$		37 889.5	
		rms dev. = 27.2 cm^{-1}	

[a] Centers of gravity were obtained from this work and Ref. 2.

[b] The parameters obtained for this free-ion calculation were: $E^1 = 7075.5$, $E^2 = 33.8$, $E^3 = 654.3$, $\xi = 2631.8$, $\alpha = 8.0$, $\beta = -764.9$; where all parameters have units of cm^{-1}.

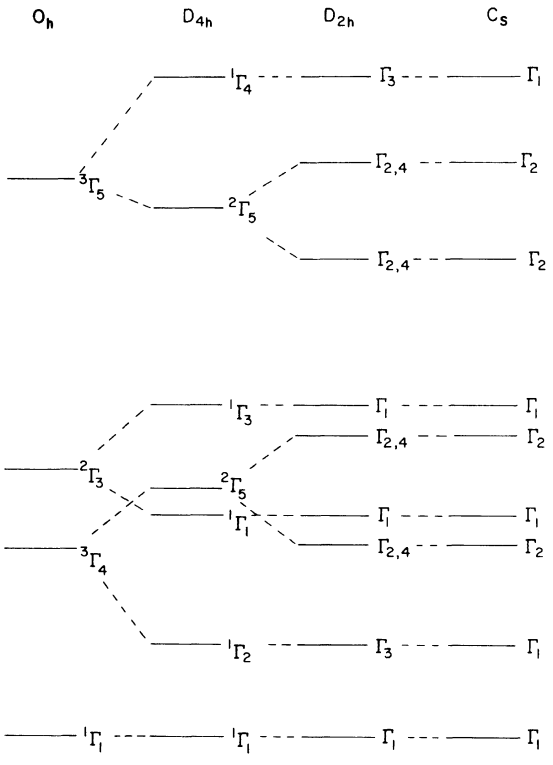

FIG. 3. Observed C_s and projected O_h, D_{4h}, and D_{2h} Stark spectrum of the $^1G_4$ manifold. The notation $\Gamma_{2,4}$ means either Γ_2 or Γ_4.

90°, in this case $\beta = 91.6°$. The D_{2h} Hamiltonian, Eq. (10), has nine adjustable parameters, however, B_0^2, B_0^4, B_4^4, B_0^6, and B_4^6 were held fixed at their D_{4h} values. Thus the starting parameters for this calculation were the values obtained in the D_{4h} calculation above and zeros for the new parameters. The parameters obtained from this calculation were then used as starting parameters and the D_{2h} fit was recalculated with all nine parameters being allowed to vary. In addition, the $^3F_4$, $^3F_3$, and the $^1D_2$ manifolds were included along with the $^1G_4$ manifold in the fitting procedure. Since the irreducible representations of the Stark levels are also included in the fit, the $^3H_6$, $^3H_4$, and $^3H_5$ manifolds were not fit since complete polarization data does not exist for these levels. In addition, the polarization data which we obtained for the $^3F_2$ manifold was ambiguous and not in agreement with that obtained by Hobrock.[2] We therefore did not fit the $^3F_2$ Stark levels, although they were included in the basis. The coefficients obtained in this fit were, $B_0^2 = -469.6$ cm^{-1}, $B_2^2 = 442.8$ cm^{-1}, $B_0^4 = -905.5$ cm^{-1}, $B_2^4 = 621.2$ cm^{-1}, $B_4^4 = 578.1$ cm^{-1}, $B_0^6 = -188.6$ cm^{-1}, $B_2^6 = 200.8$ cm^{-1}, $B_4^6 = 31.0$ cm^{-1}, and $B_6^6 = 458.1$ cm^{-1} with an rms deviation of 36.1 cm^{-1}.

Finally, the parameters obtained from the D_{2h} calculation were used as starting values to fit the C_s Hamiltonian [Eq. (4)] to the experimentally observed Stark splittings of the $^3F_4$, $^3F_3$, $^1G_2$, and $^1D_2$ manifolds. Zeros were taken for the starting values of the coefficients of the imaginary terms. Again, as in all of these calculations, all manifolds were included in the basis so that the calculations were fully J mixed. The resulting values of the coefficients of the imaginary terms along with the coefficients from the D_{2h} calculation were then used as starting parameters for a C_s calculation in which all 15 parameters were allowed to vary. This final calculation thus yields the crystal-field calculation for Tm^{3+} in $YAlO_3$. The final coefficients obtained for this calculation were $B_0^2 = -434.9$ cm^{-1}, $\mathrm{Re}B_2^2 = 420.8$ cm^{-1}, $\mathrm{Im}B_2^2 = 199.4$ cm^{-1}, $B_0^4 = -691.6$ cm^{-1}, $\mathrm{Re}B_2^4 = 444.9$ cm^{-1}, $\mathrm{Im}B_2^4 = 114.2$ cm^{-1}, $\mathrm{Re}B_4^4 = 501.2$ cm^{-1}, $\mathrm{Im}B_4^4 = -389.2$ cm^{-1}, $B_0^6 = -260.4$ cm^{-1}, $\mathrm{Re}B_2^6 = 175.6$ cm^{-1}, $\mathrm{Im}B_2^6 = 229.7$ cm^{-1}, $\mathrm{Re}B_4^6 = 92.7$ cm^{-1}, $\mathrm{Im}B_4^6 = 542.4$ cm^{-1}, $\mathrm{Re}B_6^6 = 410.5$ cm^{-1}, $\mathrm{Im}B_6^6 = 113.4$ cm^{-1} with an rms deviation of 30.3 cm^{-1}. Table IV summarizes the results of the O_h, D_{4h}, D_{2h}, and C_s calculations. Table V gives the numerical results of the C_s calculation along with the observed energy levels for

TABLE IV. Crystal-field coefficients for the O_h, D_{4h}, D_{2h}, and C_s calculations.

Coefficient	O_h symmetry (cm^{-1})	D_{4h} symmetry (cm^{-1})	D_{2h} symmetry (cm^{-1})	C_s symmetry (cm^{-1})
B_0^2		−856.6	−469.6	−434.9
$\mathrm{Re}B_2^2$			442.8	420.8
$\mathrm{Im}B_2^2$				199.4
B_0^4	−1128.2	[−1128.2] [a]	−905.5	−691.6
$\mathrm{Re}B_2^4$			621.2	444.9
$\mathrm{Im}B_2^4$				114.2
$\mathrm{Re}B_4^4$		[674.2] [a]	578.1	501.2
$\mathrm{Im}B_4^4$				−389.2
B_0^6	27.9	[27.9] [a]	−188.6	−260.4
$\mathrm{Re}B_2^6$			200.8	175.6
$\mathrm{Im}B_2^6$				229.7
$\mathrm{Re}B_4^6$		[52.2] [a]	31.0	92.7
$\mathrm{Im}B_4^6$				542.4
$\mathrm{Re}B_6^6$			458.1	410.5
$\mathrm{Im}B_6^6$				113.4
rms dev.	13.4	34.7	36.1	30.3

[a] The brackets on the D_{4h} coefficients indicate that those coefficients were held fixed at the cubic value, cf. text.

TABLE V. Comparison of the experimental and calculated C_s Stark splittings from the centers of gravity in YAlO: Tm^{3+}.

Multiplet	Observed splitting (cm^{-1}) (Ref. 2)	Irred. Rep.	Observed splitting E_e (cm^{-1}) (This work)	Irred. Rep.	Calculated splitting E_c (cm^{-1}) (This work)	Irred. Rep.	$[E_e(\Gamma) - E_c(\Gamma)]$ [a] (cm^{-1})
$^3H_6$					−334.2	Γ_1	
					−303.1	Γ_2	
					−259.7	Γ_1	
					−142.7	Γ_2	
					−116.7	Γ_1	
					−2.6	Γ_1	
					0.6	Γ_2	
					51.3	Γ_1	
					89.8	Γ_2	
					236.2	Γ_2	
					256.1	Γ_1	
					257.6	Γ_2	
					267.5	Γ_1	
$^3H_4$ [b]	−180.9				−206.0	Γ_1	
	−176.2				−136.7	Γ_2	
	−89.1				−89.7	Γ_1	
	−77.3				−40.0	Γ_1	
	17.3				−36.5	Γ_2	
	37.4				27.8	Γ_1	
	126.0				112.4	Γ_2	
	157.9				180.0	Γ_2	
	184.7				188.6	Γ_1	
$^3H_5$ [b]	−189.5	Γ_2			−267.4	Γ_2	
	−185.2	Γ_1			−211.6	Γ_2	
	−128.1	Γ_2			−207.5	Γ_1	
	−105.2	Γ_1			−72.1	Γ_1	
	−73.9				−57.9	Γ_2	
	8.3				13.5	Γ_2	
	32.0				29.7	Γ_1	
	114.0				146.5	Γ_1	
	138.4				148.2	Γ_2	
	148.9				238.6	Γ_1	
	240.0				240.0	Γ_2	
$^3F_4$	−249.3	Γ_1	−252.0	Γ_1	−258.8	Γ_1	6.8
	−191.7	Γ_2	−192.6	Γ_2	−178.7	Γ_2	−13.9
	−99.5	Γ_1	−99.1	Γ_1	−85.8	Γ_1	−13.3
	−22.9	Γ_1	−24.2	Γ_1	−30.8	Γ_2	−22.9
	18.4	Γ_2	16.9	Γ_2	−1.3	Γ_1	47.7
	102.0	Γ_2	105.7	Γ_2	114.1	Γ_2	−8.4
	117.8	Γ_2	118.1	Γ_2	127.1	Γ_1	−16.2
	144.3	Γ_1	143.3	Γ_1	134.3	Γ_2	16.2
	181.2	Γ_1	184.1	Γ_1	179.9	Γ_1	4.2
$^3F_3$	−96.4	Γ_1	−96.5	Γ_1	−73.1	Γ_1	−23.4
	−66.5	Γ_2	−66.5	Γ_2	−65.9	Γ_2	−0.6
	−33.1	Γ_2	−31.8	Γ_2	−14.6	Γ_2	−17.2
	2.5	Γ_2	7.5	Γ_2	3.1	Γ_2	4.4
	49.5	Γ_1	48.2	Γ_1	22.1	Γ_1	26.1
	63.9	Γ_1	61.1	Γ_1	56.2	Γ_1	5.4
	80.0	Γ_2	77.6	Γ_2	72.2	Γ_2	5.4
$^3F_2$ [b]	−125.6	Γ_1	−127.6	(Γ_1) [c]	−97.2	Γ_1	
	−86.1	Γ_2	−66.0	Γ_2	−81.6	Γ_2	
	31.5	Γ_1	23.3	(Γ_2)	−10.8	Γ_2	
	40.9	Γ_1	39.2	Γ_1	55.8	Γ_1	
	139.3	Γ_2	131.0	(Γ_1)	133.8	Γ_1	

TABLE V. *(continued)*

Multiplet	Observed splitting (cm^{-1}) (Ref. 2)	Irred. Rep.	Observed splitting E_e (cm^{-1}) (This work)	Irred. Rep.	Calculated splitting E_c (cm^{-1}) (This work)	Irred. Rep.	$[E_e(\Gamma)-E_c(\Gamma)]$ [a] (cm^{-1})
$^1G_4$		Γ_1	−287.7	Γ_1	−289.2	Γ_1	1.5
		Γ_1	−206.5	Γ_1	−188.0	Γ_1	−18.5
		Γ_2	−114.0	Γ_2	−132.5	Γ_2	18.5
		Γ_2	−86.9	Γ_1	−77.2	Γ_1	−9.7
		Γ_1	−14.0	Γ_2	−45.1	Γ_2	31.1
		Γ_1	13.4	Γ_1	39.8	Γ_1	−26.4
		Γ_2	147.8	Γ_2	127.4	Γ_2	20.4
		Γ_1	234.8	Γ_2	270.2	Γ_2	−35.4
		Γ_2	313.0	Γ_1	294.6	Γ_1	18.4
$^1D_2$	−124.0	Γ_1	−121.6	Γ_2	−117.2	Γ_1	−12.4
	−104.4	Γ_2	−106.2	Γ_1	−109.2	Γ_2	11.0
	28.4	Γ_1	29.0	Γ_1	50.0	Γ_1	−21.0
	84.1	Γ_2	87.2	Γ_2	67.9	Γ_2	19.3
	116.1	Γ_1	111.7	Γ_1	108.5	Γ_1	3.2
					rms dev. [d] = 30.3		

[a] ΔE is only noted for those states which were fit.

[b] These multiplets were not fit because the irreducible representations were not known for all Stark components.

[c] The polarization data did not allow unambiguous assignments of the irreducible representations to be made for the states enclosed in parenthesis.

[d] Only 14 of the 15 C_s crystal-field parameters are independent. This fact has been used in determining the rms deviation from Eq. (12).

comparison. Figure 4 compares the observed and calculated splittings from center of gravity for those manifolds which were fit to the observed spectra.

V. DISCUSSION AND CONCLUSIONS

Observed polarized absorption spectra of $YAlO_3$: Tm^{3+} have been used to obtain a fully J-mixed crystal-field calculation. In fitting the crystal-field coefficients, a descending symmetries approach was used in order to obtain starting parameters for fitting the C_s Hamiltonian. In addition, the fitting procedure was constrained to give agreement between the observed and calculated irreducible representations wherever possible. Only the $^3F_4$, $^3F_3$, $^1G_4$, and $^1D_2$ manifolds were weighted in the fit, since the polarized absorption spectra for these manifolds was complete and thus their irreducible representations known.

These calculations utilized the so-called free-ion model whereby the free-ion parameters are determined by fitting the centers of gravity of the Stark multiplets. The crystal-field parameters are then determined by diagonalizing crystal-field matrices computed from the intermediate coupled free-ion vectors. One deficiency of this method is that the crystal-field shifts the positions of the

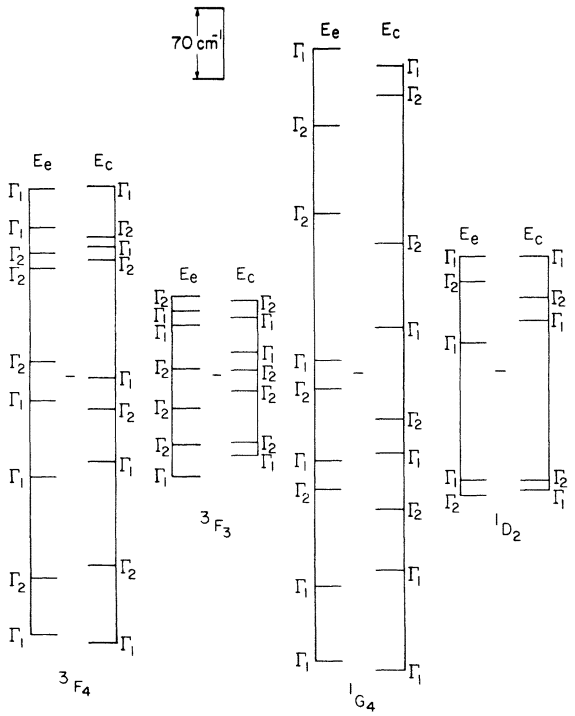

FIG. 4. Comparison of the experimental and calculated C_s Stark splittings from the centers of gravity of the $^3F_4$, $^3F_3$, $^1G_4$, and $^1D_2$ manifolds of Tm^3:YAlO. This diagram corresponds to the values given in Table V.

free-ion levels. This will have some effect on the free-ion parameters, particularly the smaller terms of Eq. (1). Crystal-field parameters calculated in this manner tend to be somewhat small in that they do not fully account for electron screening of the crystal field.

The crystal-field parameters were obtained by fitting splittings from centers of gravity rather than fitting the values of the Stark levels. The reason for fitting splittings is also owing to the fact that the crystal field causes the centers of gravity of the J manifolds to shift from their free-ion values. Since our free-ion states were fit to $YAlO_3$:Tm^{3+} spectra, they are not true free-ion levels, i.e., zero crystal field, and they implicitly contain this shift. The crystal-field calculations will still cause a shift, however, which in this case will be spurious. Thus, in the free-ion model of crystal-field calculations, if the values of the Stark levels are fit rather than their splittings from center of gravity, the B_q^k's would have to accommodate these shifts and would consequently be distorted. Some investigators[20-22] have dealt with this by using an additional parameter, E_i for each J manifold, which is added to the diagonal in order to shift the calculated groups of Stark levels to fit the observed energies. Such an approach represents an improvement only in cases where the free-ion energies of multiplets are so close together that overlapping of the Stark spectra occurs. It offers no advantage in this case where the free-ion multiplets are well separated in energy. The alternative to the free-ion model is to diagonalize the combined free-ion and crystal-field matrices and fit the free-ion and crystal-field parameters simultaneously. The free-ion parameters from such a calculation would then represent zero crystal field and the crystal-field parameters would accommodate the actual center-of-gravity shifts caused by the crystal field. Morrison *et al.*[23] have obtained the crystal field of Pr^{3+}:$LaCl_3$ by varying the free-ion and crystal-field parameters simultaneously. While their calculation yielded small changes in the free-ion and crystal-field parameters, only slight improvement in the rms deviation over the free-ion-model calculations[24] was obtained. This method of doing crystal-field calculations, although more "correct" than the free-ion model, for $YAlO_3$ would require the simultaneous fitting of a large number of parameters.

$YAlO_3$:Tm^{3+} has proven to be a very stubborn system as far as the crystal-field calculations are concerned. The rms deviation of 30.3 cm^{-1} for 26 energy differences that were fit is somewhat disappointing. Karayianis *et al.*[25] have obtained a low rms value for $YAlO_3$:Tm^{3+} by fitting the data of Antonov *et al.*[3] However, the calculation of Karayianis *et al.* was not constrained to reproduce the ordering of the irreducible representation labels. We initially tried various starting points without constraining the calculations to the irreducible representation labels of the states. In some cases we were able to improve on the rms deviation, but the results were unphysical because they did a poor job of reproducing the order of the Γ_i's in each manifold. For this reason we decided upon the descending-symmetries approach in order to obtain a good starting point for the C_s calculation.

From Table V and Fig. 4 it is seen that the agreement between the calculated and observed splittings for those levels which were fit is adequate. Of the 30 Stark levels used in the fit, agreement was obtained on the ordering of the irreducible representations for 24 of these levels. The other six levels consist of three pairs of levels for which the order of Γ_1 and Γ_2 is inverted. Of these three pairs, two of the pairs have energy separations which are very close, thus the inverted order has very little effect on the calculation. More disappointing, however, is the poor job it does for the lowest four levels of the $^3H_5$ manifold. Hobrock[2] has given the Γ_i's for four of these levels so a comparison with the calculated results is of interest. The calculations do not agree well with the splittings obtained by Hobrock[2] for this manifold. The calculated splittings are significantly higher than the observed splittings. On the other hand, most of the calculated splittings of the $^3H_4$ and $^3F_2$ manifolds are generally within the rms error when compared with the observed splittings (since the Γ_i's are not known, such a comparison assumes that the ordering of the calculated Γ_i's is correct). Also on the positive side is the fact that preliminary calculations on $YAlO_3$:Er^{3+} using the C_s $YAlO_3$:Tm^{3+} coefficients give excellent agreement with the observed $YAlO_3$:Er^{3+} splittings.[26] This will be the subject of a later paper.

In order to get better agreement with the calculated and observed splittings for the lowest four levels of the $^3H_5$ manifold we subsequently included these levels in the fitting procedure. Although it did improve the calculated splittings for those levels and gave the correct ordering for the Γ_i's, its overall effect was to degrade the calculated splittings for the other manifolds while leaving the ordering of the Γ_i's relatively in tact. Such behavior indicates that there are some strongly term (SLJ) dependent effects in the crystal field of $YAlO_3$:Tm^{3+}. Rajnak and Wybourne[27] have shown that the inability of one set of crystal field parameters to accurately reproduce the Stark splittings of all manifolds of a given crystal could be due to

the so called "electrostatically correlated crystal-field interaction." They have shown that the perturbing effects of higher-lying configurations can lead to term-dependent crystal-field coefficients, i.e., B_q^k which depend on the SLJ multiplet. If the perturbing effects of the higher-lying configurations were strong enough, it could account for the size of the rms error in this calculation. An electrostatically correlated crystal-field calculation would be of interest; however, for C_s symmetry the large number of additional parameters associated with the effective Hamiltonian would make it prohibitive.

The other alternative is that the crystal-field parameters found here represent a local minimum rather than the global minimum of $YAlO_3:Tm^{3+}$. While we would certainly have to concede that this possibility exists, we would again point out that we tried many "blind" fits from various starting points with very little success before we embarked upon the descending symmetries approach.

ACKNOWLEDGMENT

The authors would like to acknowledge the assistance of H. Ramos in taking some of the spectroscopic data for this paper.

[1]M. J. Weber, T. E. Varitimos, and B. H. Matsinger, Phys. Rev. B 8, 47 (1973).
[2]L. M. Hobrock, Ph.D. dissertation (University of Southern California, 1972) (unpublished).
[3]V. A. Antonov, P. A. Arsenev, K. E. Bienert, and A. V. Potemkin, Phys. Status Solidi A 19, 289 (1973).
[4]S. Geller and E. A. Wood, Acta. Crystallogr. 9, 1019 (1956).
[5]B. G. Wybourne, *Spectroscopic Properties of Rare Earths* (Interscience, New York, 1965).
[6]G. Racah, Phys. Rev. 76, 1352 (1949).
[7]C. W. Nielson and G. F. Koster, *Spectroscopic Coefficients for p^n and f^n Configurations* (MIT, Cambridge, Mass., 1963).
[8]H. H. Marvin, Phys. Rev. 71, 102 (1947).
[9]K. Rajnak and B. G. Wybourne, Phys. Rev. 134, A596 (1964).
[10]B. R. Judd, H. M. Crosswhite, and Hannah Crosswhite, Phys. Rev. 169, 130 (1968).
[11]B. R. Judd, Phys. Rev. 141, 4 (1966).
[12]J. M. O'Hare and V. L. Donlan, Phys. Rev. 185, 416 (1969).
[13]J. M. O'Hare, J. A. Detrio, and V. L. Donlan, J. Chem. Phys. 51, 3937 (1969).
[14]J. M. O'Hare, Phys. Rev. B 3, 3603 (1971).
[15]R. L. White and J. P. Andelin, Phys. Rev. 115, 1435 (1959).
[16]E. V. Sayre and S. Freed, J. Chem. Phys. 24, 1213 (1956).
[17]J. A. Koningstein and J. E. Geusic, Phys. Rev. 136, A711 (1964).
[18]C. A. Morrison, D. E. Wortman, and N. Karayianis, J. Phys. C 9, L191 (1976).
[19]W. T. Carnall, P. R. Fields, and K. Rajnak, J. Chem. Phys. 49, 4424 (1968).
[20]J. D. Axe and G. H. Dieke, J. Chem. Phys. 37, 2364 (1962).
[21]R. Sarup and M. H. Crozier, J. Chem. Phys. 42, 371 (1965).
[22]P. Grünberg, S. Hüfner, E. Orlich, and J. Schmitt, Phys. Rev. 184, 285 (1969).
[23]J. C. Morrison, P. R. Fields, and W. T. Carnall, Phys. Rev. B 2, 3526 (1970).
[24]J. S. Margolis, J. Chem. Phys. 35, 1367 (1961).
[25]N. Karayianis, D. E. Wortman, and C. A. Morrison, Solid State Commun. 18, 1299 (1976).
[26]V. L. Donlan and A. A. Santiago, Jr., J. Chem. Phys. 57, 4717 (1972).
[27]K. Rajnak and B. G. Wybourne, J. Chem. Phys. 41, 565 (1964).
[28]G. F. Koster, J. O. Dimmock, R. G. Wheeler, and H. Statz, *Properties of the Thirty-Two Point Groups* (MIT, Cambridge, Mass., 1963).

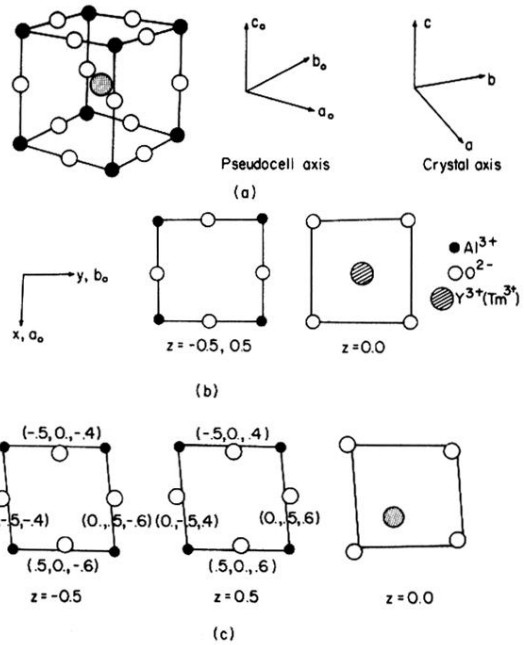

FIG. 2. (a) Relative orientation of crystal axis and pseudocell axis in $YAlO_3$. (b) The $YAlO_3$ pseudocell in the cubic approximation, $a_0 = b_0 = c_0 = 3.71$ Å and $\alpha = \beta = \gamma = 90°$. In the D_{4h} approximation, $a_0 = b_0 \neq c_0 = 3.685$ Å and $\alpha = \beta = \gamma = 90°$. In the D_{2h} approximation, $a_0 = b_0 \neq c_0 = 3.685$ Å and $\beta = 91.6°$. The two rightmost figures show X-Y planes at $Z = -\frac{1}{2}, \frac{1}{2}$, and 0 in the cubic approximation. (c) X-Y planes of the $YAlO_3$ pseudocell with C_s symmetry, $a_0 = b_0 \neq c_0$, $\beta = 91.6°$, and the Y^3 ion and O^{2-} ions displaced.